Postprint of: Szociński M., Darowicki K., Sensing the onset of epoxy coating degradation with combined Raman spectroscopy/atomic force microscopy/ electrochemical impedance spectroscopy, PROGRESS IN ORGANIC COATINGS Vol. 174 (2023), 107302, DOI: 10.1016/j.porgcoat.2022.107302

SENSING THE ONSET OF EPOXY COATING DEGRADATION WITH COMBINED RAMAN SPECTROSCOPY/ ATOMIC FORCE MICROSCOPY/ ELECTROCHEMICAL IMPEDANCE SPECTROSCOPY

M. Szociński*, K. Darowicki

Gdansk University of Technology, Faculty of Chemistry,

Department of Electrochemistry, Corrosion and Materials Engineering

G. Narutowicza Str. 11/12, Gdansk 80-233, POLAND

Abstract

The paper presents the results of investigation on epoxy resin durability upon 12-week exposure to UV radiation. The aim was early determination of the onset of epoxy degradation and for this purpose an epoxy film on steel substrate systems were periodically inspected using Raman spectroscopy, atomic force microscopy and electrochemical impedance spectroscopy. The behaviour of examined polymer could be divided into three periods: immunity, degradation initiation and failure. Early degradation initiation could be sensed only with Raman spectroscopy and AFM topography imaging where decrease in intensity of particular Raman peaks and discrete changes in topography constituted the fingerprints of UV-induced changes. At this stage electrochemical impedance spectroscopy and local dc current mapping with AFM did not provide any signs of forthcoming degradation since the epoxy film still exhibited sufficient barrier properties. Obtained results can be helpful in

*Corresponding author. Phone: +48 58 348-63-96 Fax: +48 58 347-10-92
E-mail: micszoci@pg.edu.pl

proper selection of investigation techniques in the situations where precise evaluation of polymer degradation onset is of key importance.

Keywords: epoxy resin; Raman spectroscopy; AFM; EIS; UV degradation

1. Introduction

Epoxy resins are the materials commonly used in numerous practical fields, including adhesives, laminates, polymer-matrix composites or impregnants. Broad scope of application is connected with insulating and barrier properties of epoxy resins, which make them a perfect candidate for protective coatings for metal, concrete, wood or even glass substrates. Their purpose it to isolate the substrate from the impact of ambient factors, such as water and moisture, temperature and its variations, chemical agents, mechanical factors and abrasive action of the environment.

Evaluation of the performance and durability of epoxy film under the aforementioned threats is of vital importance from the standpoint of coating durability prediction. Ultraviolet (UV) radiation is the factor having a detrimental effect on epoxy resins, where discoloration and chalking are the most typical symptoms. Longer and more intense exposure to UV radiation results in severe degradation resulting in loss of protective properties of the epoxy coatings. An important information for the user of epoxy material is whether its degradation impaired barrier properties of the coating or one deals with initial stage of degradation (with effects being only aesthetic, for instance). To achieve this goal, the authors propose to combine Raman spectroscopy, atomic force microscopy in topography and spreading resistance measurement modes and electrochemical impedance spectroscopy to evaluate UV radiation

impact on epoxy resin. These techniques have already found application in the field epoxy materials testing but not in such a combination and for the purpose highlighted in this paper. Raman spectroscopy alongside IR spectroscopy were employed for prediction of durability and elaboration of oxidation mechanism upon exposure in a photodegradation device and separately in a forced-air circulation oven at 140 °C of an industrial epoxy vinyl ester resin used in a contemporary art sculpture [1]. Fu et al. used Raman spectroscopy, SEM, and FTIR to analyse the surface morphology changes, chemical changes, stress distribution, and the deterioration of mechanical properties of a carbon fibre/epoxy microdroplet composite under UV-light irradiation intensity for 1000 hours [2]. They identified appearance of tiny particles on the surface of the composite, its discoloration and loss of mechanical properties after particular exposure times. Raman spectroscopy was also utilized to evaluate improvements introduced into epoxy-based material, for instance ammonium grafted graphene oxide added as a co-dispersant to decease the intrinsic mismatch between epoxy resin and amine curing agents during the formation of aqueous epoxy resin [3]. Localization and stratification of a mixture of epoxy/silicone resins, a curing agent and either iron oxide or calcium carbonate as fire retardant filler in a fire protective coating was investigated by Beaugendre and co-workers with Raman spectroscopy [4].

Regarding atomic force microscopy, Mailhot et al. utilized the AFM nanoindentations to identify a decrease in stiffness of epoxy/amine resin suffering from photooxidation, photolysis (in absence of oxygen) and thermooxidation [5]. Similarly, Dupuis and others employed AFM with nanomechanical mapping mode for linseed oil based epoxy resin irradiated with UV to show that the crosslinking reactions control the changes in mechanical properties of the top surface at short irradiation times (<150 h) while the β scission reactions become more competitive for long irradiation times and result in a decrease in stiffness of the surface [6]. A

combination of AFM for collection of topography images and FTIR spectra was used to compare microstructure and morphology of amine-cured epoxy coatings before and after outdoor UV exposure [7]. AFM nanoindentation allowed identification of under-crosslinked regions in the glass fibre/epoxy composite subjected to accelerated weathering tests (UV chamber and hygrothermal ageing) and natural weathering conditions in tropical climate [8]. Larche et al. provided an update on the procedures that are currently used to evaluate the photo-oxidative degradation of polymers on different scales and to characterise their durability, in particular IR spectroscopy, thermoporosimetry, DMA, AFM nanoindentation and micro-hardness determinations [9]. AFM indentation based force mapping was also the method of choice by Mishra et al. to investigate the photocatalytic degradation on the interphase region of carbon fibre composites due to ultraviolet exposure [10]. Electrochemical impedance spectroscopy (EIS) was used to evaluate degradation of carbon black/ epoxy nanocomposite coatings subjected to ultraviolet exposure followed by immersion in 3.5% NaCl solution [11]. Addition of carbon black contributed to a decrease in degradation of the coatings by absorbing UV radiation and limitation of the occurrence of microcracks on the surface of the coatings. Liu and co-workers followed evolution of barrier properties of a polyamide-cured epoxy coating during ultraviolet A photo-oxidative aging [12]. With longer exposure, EIS results show that barrier properties of the coating can be improved, which is a result of the formation of the denser surface layer due to radical recombination during UV exposure. Silicone-modified epoxy coating reinforced with various fractions of SiO_2, TiO_2, and $TiSiO_4$ nanoparticles was exposed to static electrolyte immersion, dynamic electrolyte immersion and UV exposure conditions, respectively, and evaluated with EIS for its protective properties [13].

Raman spectroscopy was used for evaluation of functionalization of graphene to enhance its compatibility with epoxy resin anticorrosive coating, which performance was then measured with electrochemical impedance spectroscopy [14]. Enhanced corrosion protection of obtained waterborne composite coating showed their high potential in marine corrosion protection. Raman spectroscopy, atomic force microscopy and electrochemical impedance spectroscopy are the tools employed by Ma et al. in investigation of performance of chemically modified graphene oxide in polyurethane acrylate coating [15]. The former two techniques were used to verify the structure of graphene oxide following the modification, while EIS was utilized to evaluate anticorrosion protection offered by the coating upon immersion in 3.5% NaCl solution. In a similar way, these three techniques were taken advantage of during examination of graphene oxide-based nanofillers and their impact on the anticorrosion performance of epoxy coating in saline medium [16].

An increasing interest is focused on portable, handheld Raman spectrometers. One of the fields of their application is the identification and conservation of historical artifacts. Synthetic polymers, based on vinyl as well as on ethyl methacrylate/methacrylate copolymer, used in the conservation of plasters were detected with portable Raman spectrometers [17]. Moreover, the minimum thickness of the polymer for successful and reliable detection was estimated to be ca. 50μm. A review on portable Raman spectrometers, including cultural heritage applications, was prepared by Jehlicka and Culka [18]. Portable Raman devices are also employed for the identification of the composition of everyday use items, for instance, a handheld Raman spectrometer occurred to be sensitive enough for initial screening of new and aged Lego® bricks made of ABS concerning constituent polymer matrices and major colour components [19]. However, to our best knowledge, there are no reports on the application of handheld Raman instruments to an investigation of protective paint coatings.

The literature review indicates there is room and need for diagnostic tools, which would allow early warning of polymer coating degradation. This fact became our motivation to elaborate the approach based on the combined implementation of Raman spectroscopy, AFM microscopy, and electrochemical impedance spectroscopy to identify the onset and evaluate the progress of polymer film degradation. Such a combination has not been applied for this purpose so far, which provides a novelty aspect to the investigation. Since this is the first attempt to combine Raman, AFM, and EIS techniques in the quest for early degradation signs, the investigations involved a relatively simple, defined epoxy resin/amine hardener system. The novelty is also reflected in discrimination between the initial discreet degradation stage, which does not discard the epoxy from further service as a protective film, and severe degradation resulting in loss of the barrier properties.

2. Materials and methods

The investigations were carried out on Epidian 5 epoxy resin (obtained from bisphenol A and epichlorohydrin, epoxide equivalent 0,48 mol/100 g) mixed with Z1 hardener (triethylenetetramine) at 100:12 weight ratio, respectively [20]. This type of epoxy is commonly used as an adhesive, laminate, impregnant and coating for various materials, including conformal coatings over electronic parts. The polymer was applied on St3 steel substrate panels using a bar applicator to obtain uniform coating. Average coating thickness, measured at 20 points randomly distributed over the specimens surface, was 42±3 μm. Prior to coating application, the substrate was cleaned and degreased with acetone. After coating deposition, the samples were left in ambient laboratory conditions for 20 days to achieve ready-for-use condition as declared by the manufacturer. Then the investigations with Raman spectroscopy, atomic force microscopy and electrochemical impedance spectroscopy were

carried out to establish initial parameters of the intact epoxy coating. In the next step coating/steel substrate samples were subjected to UV radiation exposure in a chamber equipped with 320 nm wavelength UV lamp providing a radiation intensity of 3.6 W/m^2 at a distance of 1 m. The total exposure time was equal to 12 weeks. Every 7 days the samples were removed from the chamber and subjected to periodical examination with Raman spectroscopy, AFM and EIS. Since EIS was conducted upon electrolyte immersion, each next measurement (after another 7 days of exposure) has been carried out at a different location on the sample's surface. In this way, a synergistic effect of UV and solution impact on the coating has been avoided.

Raman spectroscopy measurements

Raman spectroscopy tests were conducted using the LabRam Aramis spectrometer by Horiba Scientific Co. using the wavelength of 532nm under the ambient atmosphere. The spectral acquisition times were 5 scans accumulated with 10 sec/scan. Each time 10 spots distributed over the surface of the specimens were tested to ensure representativeness of the results.

Atomic force microscopy measurements

AFM measurements were carried out with the SPM Ntegra Aura system by NT-MDT Co.. The scans were performed in ambient conditions. The maximum available scan area was 90μmx90μm. A conductive AFM probe coated with 20-30nm thick Pt layer was employed for scanning by the tip mode. Scanning frequency amounted 0.5Hz. Acquisition, processing and analysis of the AFM images were performed with the Nova software by NT-MDT Co.. Atomic force microscopy investigations involved collection of the topographical surface images as well as spreading resistance imaging. The later was aimed at local electrical characterization of the epoxy coating. For that purpose, a bias dc voltage of 60mV was

applied between the conductive AFM tip and the coated steel substrate. The current flowing was recorded during the sample surface scan where its increments indicted defected sites. Presented AFM images are the exemplary ones selected among about 20 scans collected at various locations on the surface of each sample during each periodical examination (following every 7 days of UV exposure). These images were chosen to illustrate a dominant form of topography as well as electrical activity measured at a particular stage of exposure.

Electrochemical impedance spectroscopy measurements

Electrochemical impedance spectroscopy measurements were conducted using a two-electrode system where the steel substrate with epoxy coating constituted a working electrode and platinum mesh served as a counter electrode. The measurements were performed upon immersion in 1% NaCl solution. The surface area of the sample, confined by a PVC cylinder filled with the electrolyte, which was the examined region amounted 5cm^2. The experimental set-up included the Schlumberger 1255 frequency response analyser coupled to the high input impedance buffer Atlas 9181. Impedance spectra were recorded in the frequency range from 1MHz to 1mHz. Ten points per each frequency decade were collected. The perturbation signal amplitude was equal 40mV.

3. Results and discussion

The initial condition of the cured epoxy film on steel was evaluated prior to UV exposure with three techniques: electrochemical impedance spectroscopy, atomic force microscopy and Raman spectroscopy. Fig. 1 shows impedance spectrum in Nyquist format of the intact epoxy coating. There is a single time constant and recorded impedance is of GΩ order, which is characteristic for high-barrier coatings [21].

a)

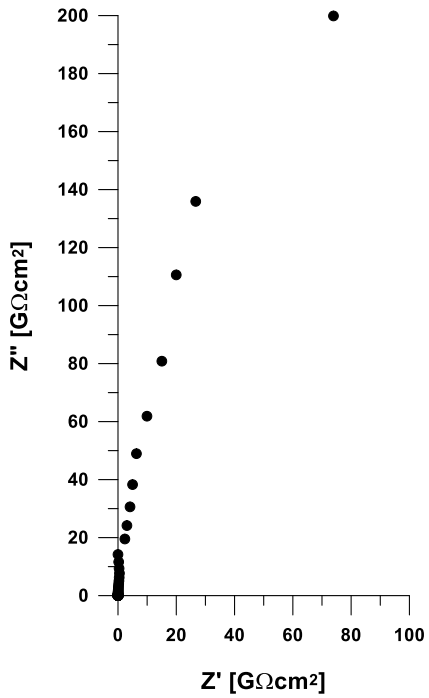

b)

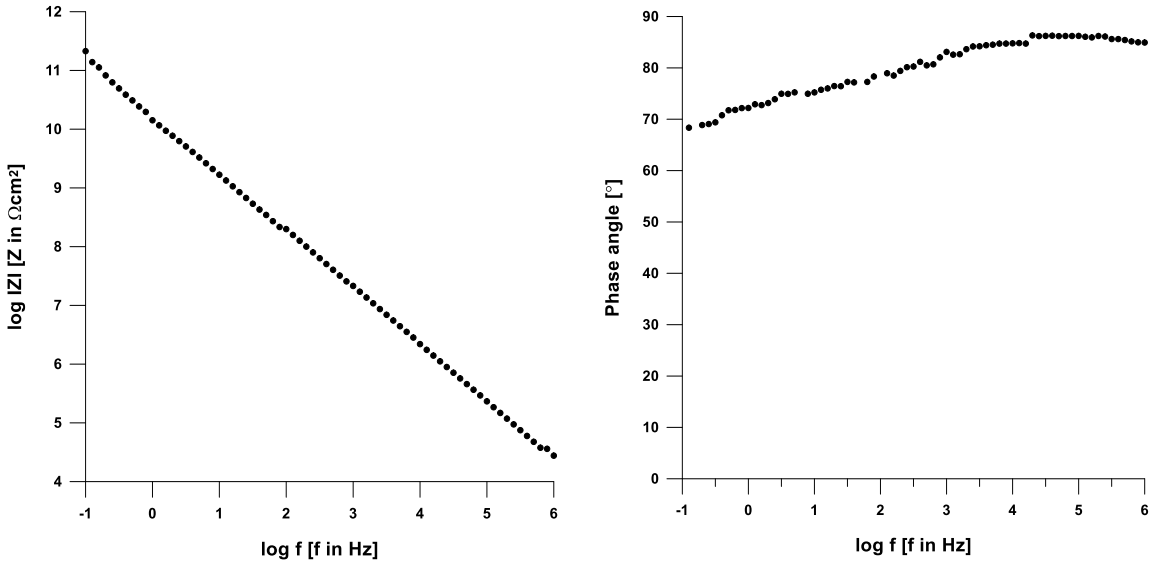

Fig. 1. Impedance spectra for the intact epoxy coating on steel substrate: (a) Nyquist format, (b) Bode format.

AFM topographical and dc current images (Fig. 2a,b) also show relatively uniform surface (average roughness equal 1.02μm, maximum height difference 2.03μm) free of any significant elevations and depressions. Dc current flowing between the AFM tip and epoxy coated steel substrate is negligibly low, in the range of a few pA, which confirms excellent insulating barrier properties of the polymer film.

a) b)

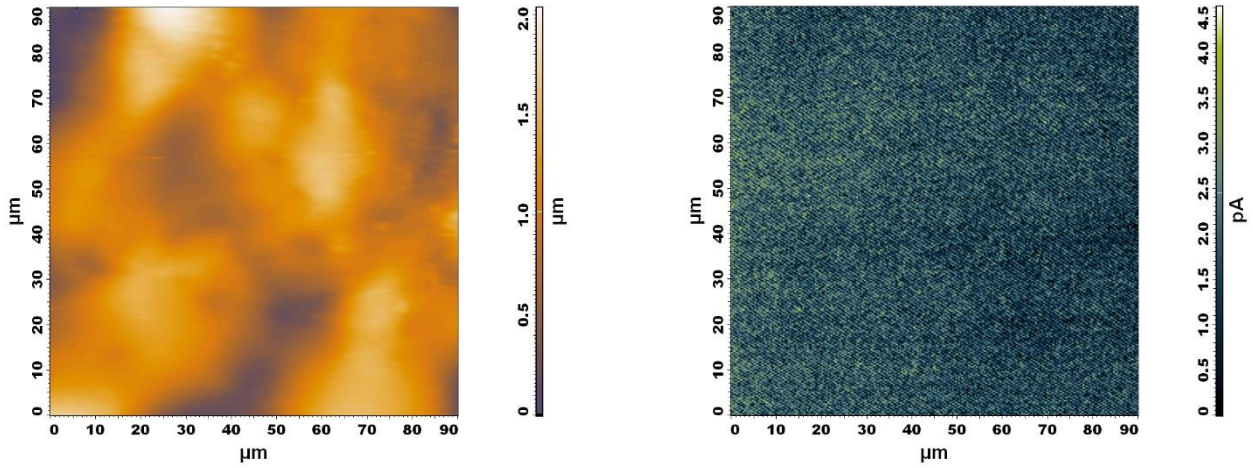

Fig. 2. Exemplary AFM topographical (a) and dc current map (b) images for the intact epoxy coating on steel substrate.

Fig. 3 presents exemplary Raman spectra collected at various stages of the investigation including the spectrum for the as-received epoxy film as well as the spectrum for the epoxy coating following a 6-week exposure to UV radiation (degradation initiation stage) and the spectrum for the epoxy coating after 12-week exposure to UV radiation (degradation stage).

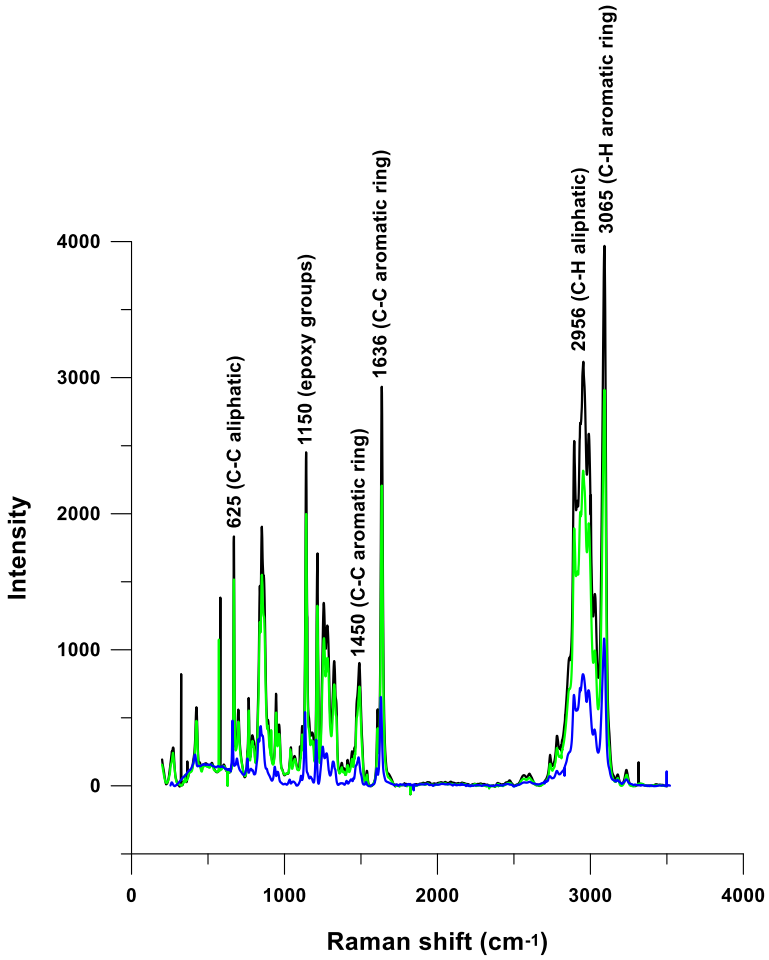

Fig. 3. Exemplary Raman spectra collected at various stages of investigation: (black) as-received epoxy film, (green) epoxy coating after 6-week exposure to UV radiation (degradation initiation stage), (blue) epoxy coating after 12-week exposure to UV radiation (degradation stage).

On the Raman spectra there are a few distinct peaks corresponding to C-H in aromatic ring (3065cm^{-1}), C-H aliphatic (2956cm^{-1}), C-C in aromatic ring (1636cm^{-1} and 1450cm^{-1}), epoxy groups (1150cm^{-1}) and C-C aliphatic (625cm^{-1}) [22]. The presence of the epoxy peak is connected with incomplete cure due to slowly progressing epoxy-amine reaction under ambient conditions. This is confirmed by a slow gradual decrease in intensity of the peak during the entire exposure time.

The condition of the epoxy film maintained stable for about 5 weeks of the exposure to ultraviolet radiation, which was confirmed by periodical inspection with EIS, AFM and Raman techniques. The coating revealed strong barrier properties in impedance investigations (coating resistance of a few hundred GΩ order) as well as in atomic force microscopy tests (unaltered topographical images and local dc current maps showing uniform non-conductive film). Intensities of particular aforementioned peaks on Raman spectra remained approximately constant throughout the initial 5 weeks of irradiation.

The first more pronounced changes occurred in the Raman spectrum recorded after 6 weeks of exposure (Fig. 3) manifested by a decrease in the intensity of the peaks attributed to stretching vibrations of C-H in aromatic ring, C-H aliphatic, C-C in aromatic ring and slightly to C-C aliphatic. This effect was accompanied by the appearance of local point-shaped depressions on the topographical AFM images illustrated in Fig. 4a. There are also tiny cracks running between most of these points. As far as barrier properties of the epoxy coating are concerned, the film is still tight and isolates metallic substrate from the ambient environment. This conclusion stems from both local dc current maps acquired with the AFM-approach as well as electrochemical impedance spectra. The former measurement showed no spots of higher dc current flow over the examined surface (Fig. 4b), while the later investigations resulted in single time constant impedance spectra yielding the coating impedance of ca. a few tens GΩ (Fig. 5), which still means a good insulating coating.

The above mentioned epoxy film characteristics continued for another four weeks of UV exposure. Based on Raman and AFM topography data it can be stated that it was the degradation initiation stage. It engulfed onset of breakdown of particular bond types in the polymer structure, which induced microscopic defects in epoxy film. Nevertheless, the

magnitude of energy accepted till that moment of exposure was not sufficient to alter barrier properties of the coating.

a) b)

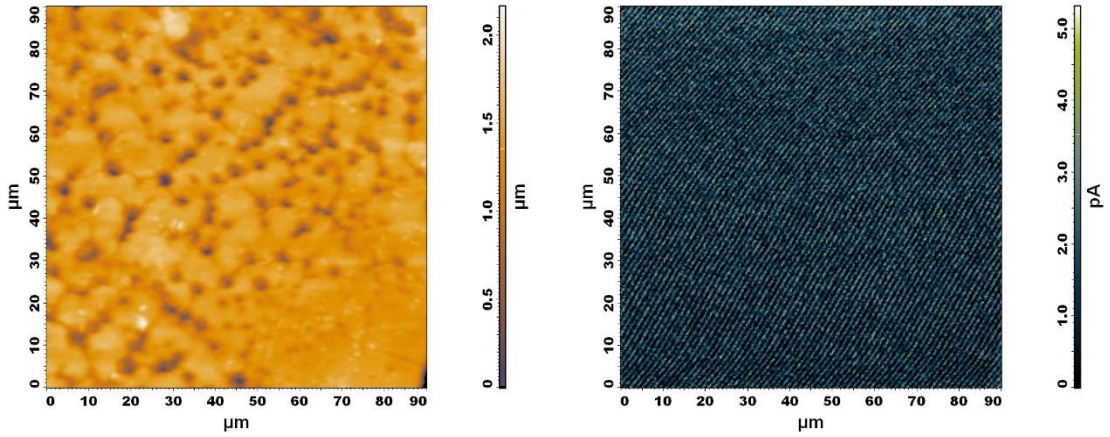

Fig. 4. Exemplary AFM topographical (a) and dc current map (b) images during degradation initiation for the epoxy coating on steel substrate following 6-week exposure to UV radiation (degradation initiation stage).

a)

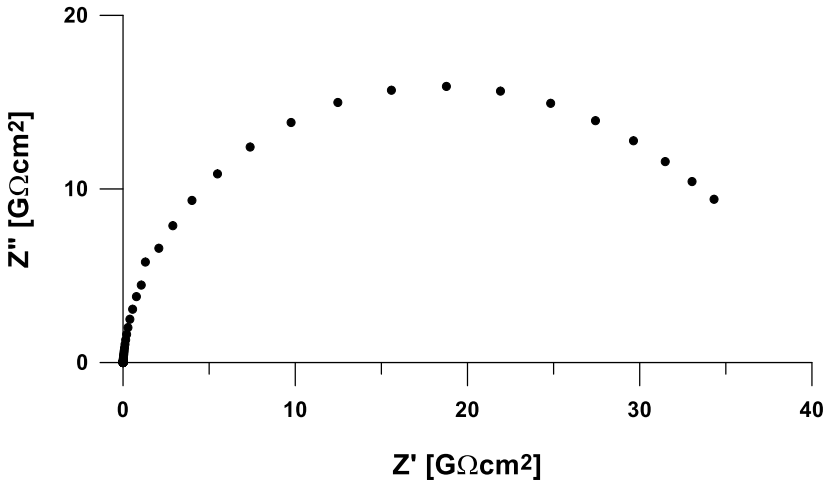

b)

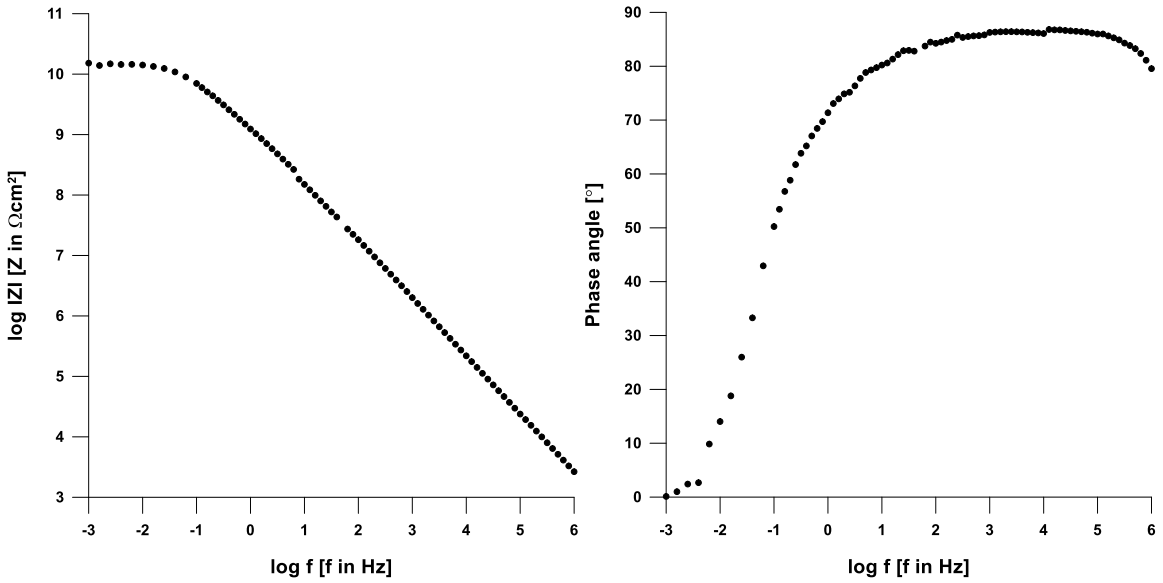

Fig. 5. Impedance spectra for the epoxy coating on steel substrate following 6-week exposure to UV radiation (degradation initiation stage): (a) Nyquist format, (b) Bode format.

The results obtained after 12 weeks of UV exposure unequivocally identified photo-induced degradation of the epoxy film. Fig. 3 depicts that the intensities of all the peaks identified on Raman spectrum decreased by more than two times indicating significant damage of particular bonds within the polymer. Following the radical model of photodegradation, polymer chains undergo scission via photoinitiation and propagation phenomena; possibly forming free hyperoxide radicals are capable of detaching hydrogen atoms resulting in cracking and fragmentation of the polymer. Epoxy coating topography shows big cracks running between and through numerous local point defects, which is visible in Fig. 6a. Moreover, there is substantial current flowing through these cracks and through bigger point defects (Fig. 6b). The magnitude of current is three orders of magnitude higher than at the beginning of the exposure as well as during the degradation initiation stage (nA vs. pA). This is the evidence of presence of through-the-coating defects, which results in loss of film tightness. It is confirmed by EIS measurements – recorded impedance spectrum reveals two time constants where the low frequency one is indicative for electrochemical reaction occurring on the substrate (Fig. 7). The coating resistance assessed based on the impedance spectrum is of kΩ order, which means the epoxy film does not constitute a barrier for corrosive agents and they can penetrate down to the metallic substrate. A significant deterioration of the protective properties of the coating could be associated with a release of stress accumulated during UV exposure. Energy absorbed during irradiation achieved a critical threshold level leading to significant structural changes of the polymer, like cracking and fragmentation.

a) b)

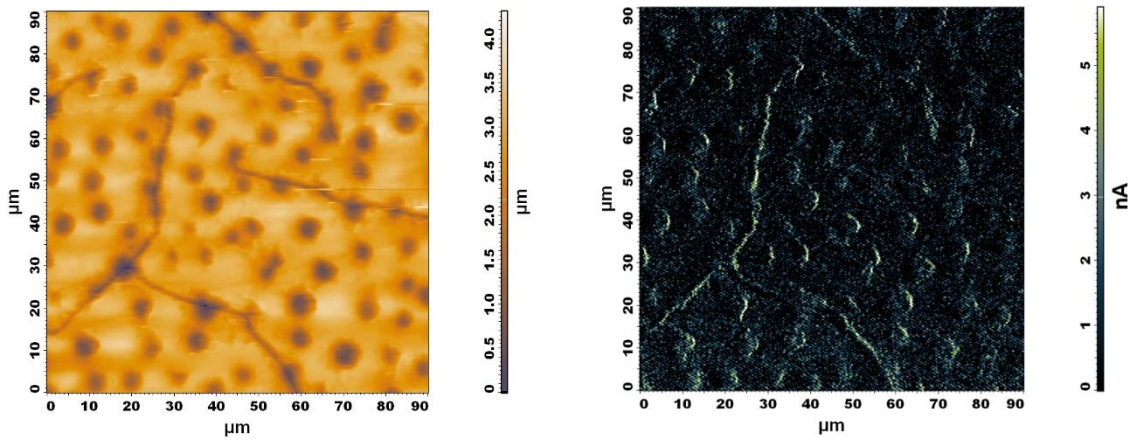

Fig. 6. Exemplary AFM topographical (a) and dc current map (b) images for the epoxy coating on steel substrate after 12-week exposure to UV radiation (degradation stage).

a)

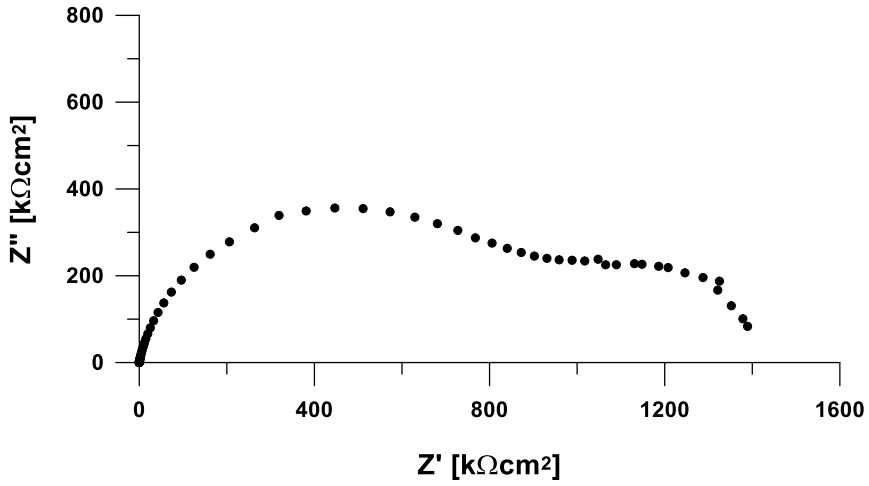

b)

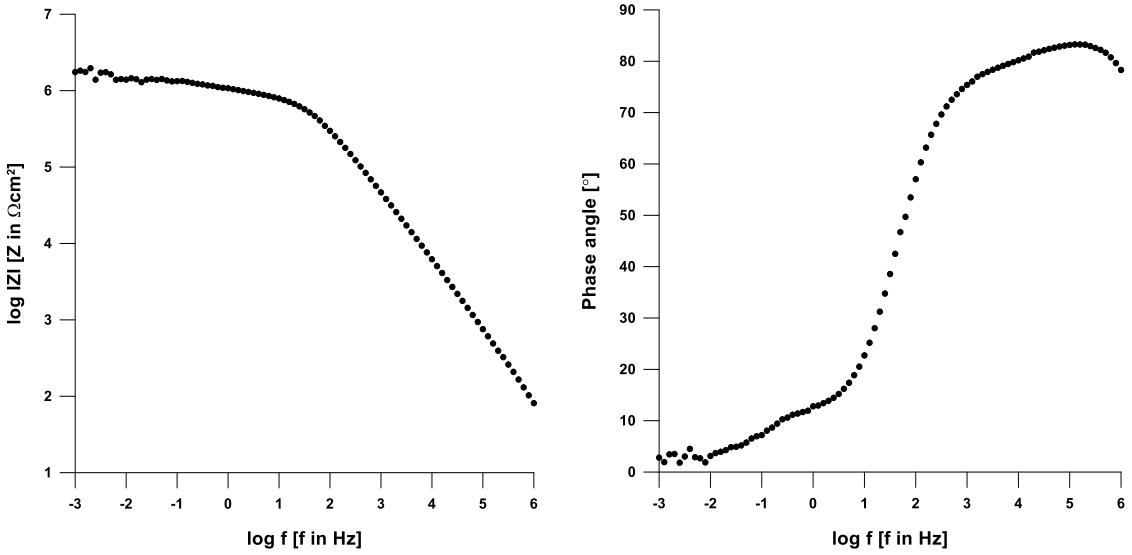

Fig. 7. Impedance spectra for the epoxy coating on steel substrate after 12-week exposure to UV radiation (degradation stage): (a) Nyquist format, (b) Bode format.

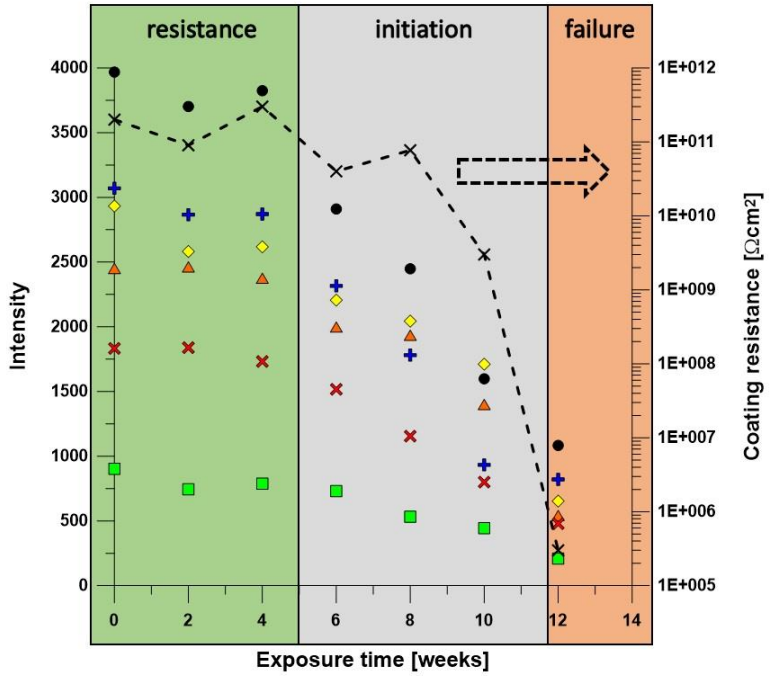

Fig. 8. Changes of intensity of particular Raman peaks during exposure of epoxy coating to UV radiation: (●) 3065cm^{-1} C-H in aromatic ring, (✚) 2956cm^{-1} C-H aliphatic, (◆) 1636cm^{-1} C-C in aromatic ring, (■) 1450cm^{-1} C-C in aromatic ring, (▲) 1150cm^{-1} epoxy groups, (✖) 625cm^{-1} C-C aliphatic. Symbol (✕) and dashed line represent evolution of the coating resistance obtained with EIS measurements.

Fig. 8 is an illustration of changes in particular Raman peaks intensity over the exposure time. Additionally, it includes evolution of epoxy coating resistance determined from electrochemical impedance spectra using the electrical equivalent circuits shown in Fig. 9.

a) b)

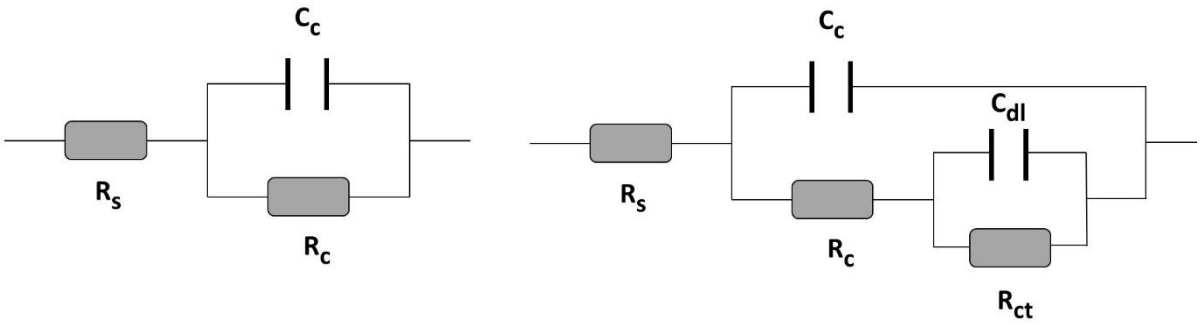

Fig. 9. Electrical equivalent circuits employed for modelling of obtained impedance spectra: a) circuit for the barrier coating, b) circuit for the defected coating, where R_s – solution resistance, R_c – coating resistance, R_{ct} – charge transfer resistance, C_c – coating capacitance, C_{dl} – electrical double layer capacitance.

Comparison and analysis of the characteristics gathered in Fig. 8 allows identification of three time regions. The first one spreads over initial 5 weeks of exposure where intensity of C-H in aromatic ring, C-H aliphatic, C-C in aromatic ring, C-C in aromatic ring, epoxy groups and C-C aliphatic peaks is at about the same level regarding each particular stretching vibration. It is consistent with high coating impedance recorded during that time. This is the region corresponding to immunity of epoxy film to UV radiation impact where no structural changes take place. The second period extends from 6^{th} to 10^{th} week of exposure and can be associated with onset of epoxy degradation. It can be sensed only with Raman spectroscopy and AFM topography investigations, which are sensitive enough to detect early stages of epoxy film degradation. At this stage the coating is still tight, without any down-to-the-substrate defects, so electrochemical impedance spectroscopy and local dc current mapping

do not provide any information about epoxy degradation onset. The changes occur on the surface and in the top layer of the coating, which as first are exposed to the external degradation factor. Hence, degradation starts at the surface, which was confirmed by the data from Raman and AFM topography examinations. In this way, the objective of the paper – identification of early signs of degradation – has been achieved. In fact, the properties and behaviour of polymer film can differ between surface and bulk. Bulk degradation mechanism of the coating at later stages was not within the scope of this paper. Nevertheless, the surface morphology changes detected after 6 weeks of exposure turned into through-the-coating defects at longer UV irradiation, which was confirmed by EIS and AFM local dc current mapping. In this way, surface behaviour also translated in bulk degradation. This third stage of coating response to UV exposure occurs after 10 weeks where all applied techniques consistently indicate critical epoxy degradation, which does not constitute a barrier protecting metallic substrate any more.

Summarizing, proposed approach employing Raman and AFM techniques proved advantageous and can be of potential application in case early detection and spatial localization of defects in polymer films is a concern.

4. Conclusions

The employed combination of Raman spectroscopy, atomic force microscopy, and electrochemical impedance spectroscopy allowed discrimination of three stages of epoxy film response to UV irradiation: resistance, degradation initiation, and failure. Degradation initiation could be identified only by a decrease in intensity of particular Raman peaks and by local depressions on AFM topography images. At this stage the epoxy coating maintained its insulating properties. Failure was identified with EIS and local dc current mapping, which revealed formation of through-the-defects. Performed investigations show that subtle changes in particular Raman peaks and AFM surface topography precede the changes in capacitive-resistive properties detectable by electrochemical impedance and dc current mapping. Thus, such a combination of techniques allows early detection of degradation and more complete evaluation of the condition of epoxy films exposed to UV radiation.

5. References

[1] Rodriguez-Mella Y, López-Morán T, López-Quintela M A, Lazzari M. Durability of an industrial epoxy vinyl ester resin used for the fabrication of a contemporary art sculpture. Polym Degrad Stab 2014; (107): 277-284. http://dx.doi.org/10.1016/j.polymdegradstab.2014.02.008

[2] Fu X, Yi D, Tan C, Wang B. Micromechanics analysis of carbon fiber/epoxy microdroplet composite under UV light irradiation by micro-Raman spectroscopy. Polym Compos 2020; (41): 2154–2168. DOI: 10.1002/pc.25528

[3] Tian Y, Xie Y, Dai F, Huang H, Zhong L, Zhang X. Ammonium-grafted graphene oxide for enhanced corrosion resistance of waterborne epoxy coatings. Surf Coat 2020; (383): 125227. https://doi.org/10.1016/j.surfcoat.2019.125227

[4] Beaugendre A, Lemesle C, Bellayer S, Degoutin S, Duquesne S, Casetta M, Pierlot C, Jaime F, Kim T, Jimenez M. Flame retardant and weathering resistant self-layering epoxy-silicone coatings for plastics. Prog Org Coat 2019; (136): 105269. https://doi.org/10.1016/j.porgcoat.2019.105269

[5] Mailhot B, Morlat-Therias S, Bussiere P-O, Gardette J-L. Study of the degradation of an epoxy/amine resin, 2 kinetics and depth-profiles. Macromol Chem Phys 2005; (206): 585–591. DOI: 10.1002/macp.200400394

[6] Dupuis A, Perrin F-X, Torres A U, Habas J-P, Belec L, Chailan J-F. Photo-oxidative degradation behavior of linseed oil based epoxy resin. Polym Degrad Stab 2017; (135): 73-84. http://dx.doi.org/10.1016/j.polymdegradstab.2016.11.021

[7] Gu X, Nguyen T, Oudina M, Martin D, Kidah B, Jasmin J, Rezig A, Sung L, Byrd E, Martin J W, Ho D L, Jean Y C. Microstructure and morphology of amine-cured epoxy coatings before and after outdoor exposures – an AFM study. JCT Research 2005; (2): 547-556.

[8] Belec L, Nguyen T H, Nguyen D L, Chailan J F. Comparative effects of humid tropical weathering and artificial ageing on a model composite properties from nano- to macro-scale. Compos Part A 2015; (68) 235-241. http://dx.doi.org/10.1016/j.compositesa.2014.09.028

[9] Larche J-F, Bussiere P-O, Therias S, Gardette J-L. Photooxidation of polymers: relating material properties to chemical changes. Polym Degrad Stab 2012; (97): 25-34. doi:10.1016/j.polymdegradstab.2011.10.020

[10] Mishra K, Babu L K, Singh R. Characterization of UV degraded carbon fiber-matrix interphase using AFM indentation. in Mechanics of Composite and Multi-functional Materials, Volume 6, Proceedings of the 2017 Annual Conference on Experimental and Applied Mechanics, Springer, 2018. p. 175.

[11] Ghasemi-Kahrizsangi A, Shariatpanahi H, Neshati J, Akbarinezhad E. Degradation of modified carbon black/epoxy nanocomposite coatings under ultraviolet exposure. Appl Surf Sci 2015; (353): 530-539. http://dx.doi.org/10.1016/j.apsusc.2015.06.029

[12] Liu F, Yin M, Xiong B, Zheng F, Mao W, Chen Z, He C, Zhao X, Fang P. Evolution of microstructure of epoxy coating during UV degradation progress studied by slow positron annihilation spectroscopy and electrochemical impedance spectroscopy. Electrochim. Acta 2014; (133): 283-293. http://dx.doi.org/10.1016/j.electacta.2014.04.002

[13] Basiru Y A, Ammar S, Ramesh K, Vengadaesvaran B, Ramesh S, Arof A K. Corrosion protection performance of nanocomposite coatings under static, UV, and dynamic conditions. J. Coat. Technol. Res. 2018; (15): 1035–1047. https://doi.org/10.1007/s11998-017-0038-z

[14] Ding J, ur Rahman O, Peng W, Dou H, Yu H. A novel hydroxyl epoxy phosphate monomer enhancing the anticorrosive performance of waterborne graphene/epoxy coatings. Appl Surf Sci 2018; (427): 981-991. http://dx.doi.org/10.1016/j.apsusc.2017.08.224

[15] Ma Y, Ye Y, Wan H, Chen L, Zhou H, Chen J. Chemical modification of graphene oxide to reinforce the corrosion protection performance of UV-curable polyurethane acrylate coating. Prog Org Coat 2020; (141): 105547. https://doi.org/10.1016/j.porgcoat.2020.105547

[16] Rajitha K, Mohana K N S. Synthesis of graphene oxide-based nanofillers and their influence on the anticorrosion performance of epoxy coating in saline medium. Diam Relat Mater 2020; (108): 107974. https://doi.org/10.1016/j.diamond.2020.107974

[17] Conti C, Striova J, Aliatis I, Colombo C, Greco M, Possenti E, Realini M, Brambilla L, Zerbi G. Portable Raman versus portable mid-FTIR reflectance instruments to monitor synthetic treatments used for the conservation of monument surfaces. Anal Bioanal Chem 2013; (405):1733–1741. doi: 10.1007/s00216-012-6594-2

[18] Jehlicka J, Culka A. Critical evaluation of portable Raman spectrometers: From rock outcrops and planetary analogs to cultural heritage – A review. Anal Chim Acta 2022; (1209): 339027. https://doi.org/10.1016/j.aca.2021.339027

[19] Reggio D, Saviello D, Lazzari M, Iacopino D. Characterization of contemporary and historical acrylonitrile butadiene styrene (ABS)-based objects: Pilot study for handheld

Raman analysis in collections. Spectrochim Acta A Mol Biomol Spectrosc 2020; (242): 118733. https://doi.org/10.1016/j.saa.2020.118733

[20] https://www.c-l.eu/epidian-5/ (accessed 19.05.2022)

[21] Sekine I. Recent evaluation of corrosion protective paint films by electrochemical methods. Prog Org Coat 1997; (31) 73-80. https://doi.org/10.1016/S0300-9440(97)00020-9

[22] Socrates G. Infrared and Raman Characteristic Group Frequencies. Tables and Charts, third ed., Wiley, Chichester, 2001

Figure captions

Fig. 1. Impedance spectra for the intact epoxy coating on steel substrate: (a) Nyquist format, (b) Bode format.

Fig. 2. Exemplary AFM topographical (a) and dc current map (b) images for the intact epoxy coating on steel substrate.

Fig. 3. Exemplary Raman spectra collected at various stages of investigation: (black) as-received epoxy film, (green) epoxy coating after 6-week exposure to UV radiation (degradation initiation stage), (blue) epoxy coating after 12-week exposure to UV radiation (degradation stage).

Fig. 4. Exemplary AFM topographical (a) and dc current map (b) images during degradation initiation for the epoxy coating on steel substrate following 6-week exposure to UV radiation (degradation initiation stage).

Fig. 5. Impedance spectra for the epoxy coating on steel substrate following 6-week exposure to UV radiation (degradation initiation stage) : (a) Nyquist format, (b) Bode format.

Fig. 6. Exemplary AFM topographical (a) and dc current map (b) images for the epoxy coating on steel substrate after 12-week exposure to UV radiation (degradation stage).

Fig. 7. Impedance spectra for the epoxy coating on steel substrate after 12-week exposure to UV radiation (degradation stage): (a) Nyquist format, (b) Bode format.

Fig. 8. Changes of intensity of particular Raman peaks during exposure of epoxy coating to UV radiation: (●) 3065cm^{-1} C-H in aromatic ring, (✚) 2956cm^{-1} C-H aliphatic, (◆) 1636cm^{-1} C-C in aromatic ring, (■) 1450cm^{-1} C-C in aromatic ring, (▲) 1150cm^{-1} epoxy groups, (✖) 625cm^{-1} C-C aliphatic. Symbol (✕) and dashed line represent evolution of the coating resistance obtained with EIS measurements.

Fig. 9. Electrical equivalent circuits employed for modelling of obtained impedance spectra: b) circuit for the barrier coating, b) circuit for the defected coating, where R_s – solution resistance, R_c – coating resistance, R_{ct} – charge transfer resistance, C_c – coating capacitance, C_{dl} – electrical double layer capacitance.